Liquid Crystals
Publication details, including instructions for authors and subscription information:
http://www.informaworld.com/smpp/title~content=t713926090

Influence of the molecular length on the occurrence of incommensurate low ordered smectic phases for non-symmetric dimesogenic compounds

F. Hardouin; M. F. Achard; M. Laguerre; Jung-Il Jin; Doo-Hyun Ko

To cite this Article Hardouin, F. , Achard, M. F. , Laguerre, M. , Jin, Jung-Il and Ko, Doo-Hyun(1999) 'Influence of the molecular length on the occurrence of incommensurate low ordered smectic phases for non-symmetric dimesogenic compounds', Liquid Crystals, 26: 4, 589 — 599

To link to this Article: DOI: 10.1080/026782999205047

URL: http://dx.doi.org/10.1080/026782999205047

Liquid Crystals, 1999, Vol. 26, No. 4, 589–599

Influence of the molecular length on the occurrence of incommensurate low ordered smectic phases for non-symmetric dimesogenic compounds

F. HARDOUIN*, M. F. ACHARD, M. LAGUERRE
Centre de Recherche Paul Pascal, Université Bordeaux I, Av. A. Schweitzer,
33600 Pessac, France

JUNG-IL JIN and DOO-HYUN KO
Department of Chemistry, College of Sciences, Korea University, Seoul 136-701,
Korea

(*Received 19 August 1998; accepted 20 November 1998*)

Systematic physical chemistry studies are in progress concerning the occurrence of incommensurate low ordered smectic phases (S_{ic})† in non-symmetric dimesogens with molecular parameters varying from those of the standard compound KI-5(4). In the present study, the selected molecules possess the same cholesteryl unit and the same spacer length, but the terminal chain of the aromatic mesogenic part is varied. Up to a critical molecular length, a competition between two incommensurate lengths is observed and the dimesogenic compounds respond to the frustration connected to this competition with the formation either of an incommensurate phase S_{ic} or of a two dimensional modulated phase. For longer dimesogens, a commensurate lock-in of the two characteristic lengths systematically occurs.

1. Introduction

Of all the molecular architectures known to support liquid crystal behaviour, one attracting particular attention is the non-symmetric dimesogenic structure in which two different mesogenic moieties are linked via a flexible spacer [1–24]. For about four years, we have focused on dimesogens composed of a cholesteryl mesogenic unit and a classical unit of two aromatic rings [10, 13, 23]. The earlier results on these series showed clearly the existence of two smectic modulations: one corresponds to a layer spacing approximately half the molecular length revealing an intercalated structure, the other to a layer spacing close to or larger than the dimesogen length [13]. The condensation of one or the other of these modulations is found to depend on the length of the aliphatic spacer. In the KI-n(4) series (where n and 4 refer to the number of methylene groups in the spacer and the length of the terminal chain, respectively), the smectic layering is connected to the 'dimer' length for short spacers, while longer spacer homologues relate to an intercalated structure [13]. More surprising, is the occurrence for a specific intermediate spacer length ($n = 5$), of an incommensurate low ordered smectic phase S_{ic}, in which the two incommensurate smectic layerings coexist [10, 23]. Additional investigations on several homologues of KI-5(4)—changing the nature of the terminal chain (KII-5(4)) or the linking group between the two aromatic rings—clearly demonstrated that the occurrence of incommensurate fluid smectic phases depends on strict molecular conditions and that at the present time this behaviour remains an exception [23]. Indeed, despite the great wealth of liquid crystalline materials, KI-5(4) and KII-5(4) are the only two examples exhibiting incommensurate fluid S_{ic} phases.

By comparison with other families of dimesogens for which S_{ic} phases have never been observed so far, the prime novelty of these KI compounds originates from the inclusion of a mesogenic moiety constituted by the cholesteryl part, which dictates the value of one periodicity corresponding to a 'monomer-like arrangement'. The second smectic periodicity is connected to the 'dimer' length. The initial reports concerning these families of non-symmetric dimesogens described the KI-n(4) series for which the carbon number of the terminal chain was kept constant and a lengthening of the spacer led to the disappearance of the 'dimer' periodicity. Another

---

*Author for correspondence.

†The nomenclature used by the authors in this paper is based on the smectic periodicity rather than the tilted or non-tilted nature of the phase. This system has been preserved with its use of S for smectic rather than the conventional Sm employed in the Journal (Editor).

Journal of Liquid Crystals ISSN 0267-8292 print/ISSN 1366-5855 online ©1999 Taylor & Francis Ltd
http://www.tandf.co.uk/JNLS/lct.htm
http://www.taylorandfrancis.com/JNLS/lct.htm

way to change this periodicity continuously is to vary systematically the terminal chain length *m*, keeping the spacer constant. In the present study *m* is varied from 2 to 10, in order to investigate the role of the molecular length in stabilizing incommensurate smectic phases.

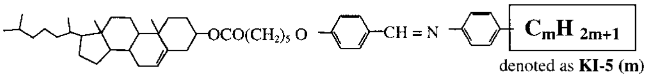

denoted as **KI-5 (m)**

2. Experimental

2.1. *Synthesis*

Synthetic details for the preparation of compound KI-5(4) were given in [10] and the same method exactly was utilized in the synthesis of all the other compounds. Special attention was paid to on purification of the materials. Moreover, since all the Schiff 's base compounds are very moisture sensitive, care was always taken to keep them in dry conditions.

2.2. *Experimental techniques*

An initial identification of the liquid crystalline phases was carried out using thermal optical microscopy (Leitz microscope equipped with a Mettler FP52 hot stage). Observations were systematically made either without surface treatment of the substrate or with rubbed polyimide as aligning agent, resulting in a planar texture. The temperature range of each phase was detected by differential scanning calorimetry (Perkin Elmer DSC7). The phase structures were determined using X-ray diffraction on powder and aligned samples. The X-ray scattering experiments were carried with an 18 kW rotating anode X-ray source (Rigaku-200) with the use of a Ge(1 1 1) crystal as monochromator. The scattered radiation was collected on a two dimensional detector (Imaging Plate system from Mar Research, Hamburg). The samples were placed in an oven, providing a temperature control of 0.1 K. Aligned samples were obtained by a surface treatment with a procedure already described [23].

2.3. *Computational methods*

2.3.1. *Molecular mechanics*

Calculations were performed on an SGI Indigo platform running MacroModel version 5.0 (Columbia University, New York) [25] or Insight II and Discover version 2.3.5 (MSI, San Diego, CA.). Conformational minima were found using the modified MM3* (1991 parameters) [26] force field as implemented and completed in the MacroModel program. Build structures were minimized to a final rms gradient $\leqslant 0.005\,\mathrm{kJ\,Å^{-1}\,mol^{-1}}$ via the Truncated Newton Conjugate Gradient (TNCG, if $N_{\mathrm{atoms}} \leqslant 250$) method (1000 cycles) or the Polak–Ribière Conjugate Gradient (PRCG, if $N_{\mathrm{atoms}} > 250$) method (2000 cycles). In all cases the extended cut-off option was used (VdW = 8 Å, electrostatic = 20 Å and H-bond = 4 Å).

2.3.2. *Stochastic dynamics simulation*

This variant of molecular dynamics (forces from the force field are augmented by frictional and random forces which simulate some of the properties of a dense medium) is implemented in MacroModel [27]. The temperature was set at 300 K and the total time of run at 100 ps (time step 1.5 fs). SHAKE algorithm was on (hydrogens only). A snap-shot was stored every ps during the run.

2.3.3. *Quantum mechanics calculations and electrostatic potentials*

The MacroModel files were converted into CSSR format using an in-house program and partial atomic charges were calculated using the MOPAC/MNDO method. Electrostatic potential maps were calculated using the VSS method via the QCPE no. 249 software [28] modified in order to use the graphic routines of MSI program Insight II. The maps were drawn within a 0.5 Å cubic grid.

3. Results and discussion

3.1. *Phase characterization*

We recall first the polymorphism of the reference compound KI-5(4) [23]:

$$\mathrm{Cr} \xrightarrow{85^{\circ}\mathrm{C}} \mathrm{S}_{\tilde{\mathrm{C}}} \xrightarrow{97^{\circ}\mathrm{C}} \mathrm{S}_{q3} \xrightarrow{141^{\circ}\mathrm{C}} \mathrm{S}_{\mathrm{ic}} \xrightarrow{146^{\circ}\mathrm{C}} \mathrm{S}_{q1\ \mathrm{LT}} \xrightarrow{152^{\circ}\mathrm{C}}$$

$$S_{q1\ \mathrm{HT}} \xrightarrow{164^{\circ}\mathrm{C}} \mathrm{TGB} \xrightarrow{168^{\circ}\mathrm{C}} \mathrm{N}^{*} \xrightarrow{192^{\circ}\mathrm{C}} \mathrm{I}$$

The nomenclature used to describe the smectic phases corresponds to a structural classification connected to the smectic periodicity rather than the tilted or non-tilted nature of the phase (C or A). This complex phase sequence results from the competition between two incommensurate smectic periodicities: $2\pi/q1$ connected to the 'dimer' length and $2\pi/q3$ associated with a 'monomer-like arrangement'. At high temperatures ($T > 146$°C), $2\pi/q1$ predominates in the different S_{q1} phases, while between 97 and 141°C, the other periodicity $2\pi/q3$ prevails in the S_{q3} phase. In addition, this system responds to the frustration connected to this competition with the formation of an incommensurate low ordered smectic phase (S_{ic} for $141^{\circ}\mathrm{C} < T < 146^{\circ}\mathrm{C}$) and, as in polar systems [29], of a two dimensional modulated phase $\mathrm{S}_{\tilde{\mathrm{C}}}$ (for $T < 97^{\circ}\mathrm{C}$).

As shown in the table, quite simple phase sequences are observed in the series of five KI-5(*m*) homologues studied here. Lengthening the terminal chain causes the clarification temperature to decrease as observed for conventional low molar mass liquid crystals. On the contrary, the cholesteric–smectic transition temperatures

Table. Transition temperature (°C) and enthalpy, ΔH, data in brackets (kJ mol^{-1}) for the KI-5(m) series. [ ] indicates a monotropic transition.

m	Phase sequence
2	$\mathrm{Cr} \xrightarrow[(17.7)]{139} \mathrm{S1} \xrightarrow[(0.56)]{157} \mathrm{N^*} \xrightarrow[(3.0)]{198} \mathrm{I}$ $[\mathrm{S2}]\ {}^{96} \hookleftarrow$
3	$\mathrm{Cr} \xrightarrow[(20.2)]{112} \mathrm{S1} \xrightarrow[(0.58)]{149} \mathrm{TGB} \xrightarrow{151} \mathrm{N^*} \xrightarrow[(3.75)]{196} \mathrm{I}$ $[\mathrm{S2}]\ {}^{98} \hookleftarrow (0.02)$
4	$\mathrm{Cr} \xrightarrow{85} \mathrm{S}_{\check{\mathrm{C}}} \xrightarrow{97} \mathrm{S}_{q}^{3} \xrightarrow{141} \mathrm{S_{ic}} \xrightarrow{146} \mathrm{S}_{q}^{1\,\mathrm{LT}} \xrightarrow{152} \mathrm{S}_{q}^{1\,\mathrm{HT}} \xrightarrow{164} \mathrm{TGB} \xrightarrow{168} \mathrm{N^*} \xrightarrow{192} \mathrm{I}$
5	$\mathrm{Cr} \xrightarrow[(26)]{70} \mathrm{S'2} \xrightarrow[(0.01^{a})]{102} \mathrm{S'1} \xrightarrow[(0.63)]{176} \mathrm{N^*} \xrightarrow[(3.73)]{190} \mathrm{I}$
6	$\mathrm{Cr} \xrightarrow[(25)]{84} \mathrm{S'2} \xrightarrow[(0.02^{a})]{112} \mathrm{S'1} \xrightarrow[(1.29)]{181} \mathrm{N^*} \xrightarrow[(3.56)]{188} \mathrm{I}$
10	$\mathrm{Cr} \xrightarrow[(36)]{84} \mathrm{S'2} \xrightarrow[(0.03^{a})]{115} \mathrm{S'1} \xrightarrow[(14)]{184} \mathrm{I}$

[a] Heat capacity discontinuity observed for the S′1–S′2 transition for longer homologues.

initially fall ($m = 2 \rightarrow 3$) before rising as m is subsequently increased. This unusual dependence of $T_{\mathrm{N^*\text{-}S}}$ on the length of the terminal alkyl chain suggests different smectic sequences for short tails ($m = 2, 3$) and for longer homologues. In this sense KI-5(4) does act as a turning point in this series.

3.1.1. *Long homologues: m = 5, 6, 10*

The longer homologues of the KI-5(m) series exhibit two smectic phases (labeled S′1 and S′2 before assignment) and behave in a similar fashion except for the direct smectic–isotropic transition for KI-5(10). The X-ray patterns of these smectic phases show a broad diffuse band in the wide angle region indicating disordered smectics (i.e. liquid-like short range order within the layers).

At low angles, the S′1 phases are characterized by a sharp reflection with one harmonic corresponding at high temperature to the wavevector $q1 = 0.146\,\text{Å}^{-1} = 2\pi/43\,\text{Å}^{-1}$ for KI-5(5), $q1 = 0.143\,\text{Å}^{-1} = 2\pi/44\,\text{Å}^{-1}$ for KI-5(6) and $q1 = 0.132\,\text{Å}^{-1} = 2\pi/47.6\,\text{Å}^{-1}$ for KI-5(10). The layer spacing d slightly decreases with temperature and is lower than the estimated all-*trans* molecular length l obtained from molecular models ($l_{\mathrm{KI\text{-}5(5)}} = 45.7\,\text{Å}$, $l_{\mathrm{KI\text{-}5(6)}} = 46.9\,\text{Å}$, $l_{\mathrm{KI\text{-}5(10)}} = 51.7\,\text{Å}$).

The patterns of the S′2 phases are characterized by one resolution-limited peak corresponding to the wavevector $q1$ with one harmonic at $2q1$. The value of $q1$ regularly increases from the values measured for S′1 to $q1 = 0.157\,\text{Å}^{-1} = 2\pi/40\,\text{Å}^{-1}$ for KI-5(5), $q1 = 0.153\,\text{Å}^{-1} = 2\pi/41\,\text{Å}^{-1}$ for KI-5(6) and $q1 = 0.136\,\text{Å}^{-1} = 2\pi/46.2\,\text{Å}^{-1}$ for KI-5(10) at low temperature.

The thermal evolution of the layer spacing in the S′1 and S′2 phases for the three homologues is shown in figure 1.

From a textural point of view, the S′1 phases show focal-conic groups and homeotropic or pseudo-homeotropic textures. On cooling, the focal-conic fans

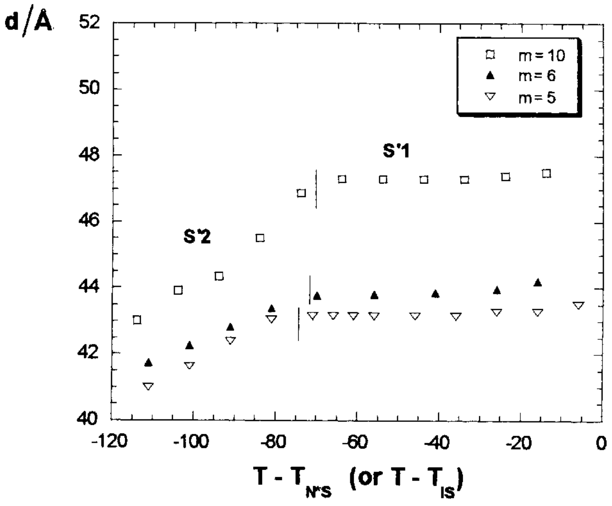

Figure 1. Evolution of the layer spacing d (Å) versus the reduced temperature $T\text{–}T_{\mathrm{N^*S}}$ (or $T\text{–}T_{\mathrm{IS}}$ for KI-5(10)).

become crossed by bars at the S′1–S′2 transition and these remain in the S′2 phase. At the same time the homeotropic domains become slightly birefringent. Thus, the S′2 phase is undoubtedly a tilted smectic. Nevertheless, the S′1 phases of the longer homologues have yet to be identified as A or C phases since the layer spacing is clearly lower than the molecular length. The problem in doing this arises because it is difficult to distinguish between aligned SmC and SmA phases and in particular an antiferroelectric structure which often appears analogous to a smectic A.

From a thermodynamic point of view, the S′1–S′2 phase change is accompanied by a heat capacity discontinuity without latent heat, suggesting a mean-field behaviour of this second order transition. This continuity of the first derivatives of the thermodynamical potential is clearly evidenced in the thermal evolution of the layer spacing in figure 1.

To summarize, longer homologues exhibit two kinds of commensurate S_{q1} phases (smectic A–smectic C or more probably smectic C–smectic C) corresponding to the smectic periodicity imposed by the ‘dimer’ length.

3.1.2. *Short homologues: m = 2, 3*

As previously mentioned, the short tail compounds of the KI-5(m) series exhibit two smectic phases which are not those of the longer compounds. Microscopic observations indicate a similar phase sequence for KI-5(2) and KI-5(3), except for the additional TGB phase for $m = 3$. In both compounds, the S1–S2 phase transition corresponds to a very weak transitional enthalpy, suggesting that the structural rearrangement involves little change in molecular ordering and no change in the symmetry. The microscopic observations corroborate this hypothesis: regions with focal-conic and homeotropic textures are both observed in S1 and S2 phases, indicating a uniaxial medium. The S1–S2 transition is revealed only by a multiplication of the focal-conic groups, suggesting a change of the layering parameter. Similar observations were made for KI-5(2), but only the S2 phase is detected under the microscope since it crystallizes rapidly on its formation.

X-ray diffraction experiments were performed on aligned samples. The S1 and S2 phases are disordered smectic phases since a broad peak centred at $2\pi/5.4\,\text{Å}^{-1}$ is typical of the liquid-like short range order within the layers. In the low angle region, the S1 phases of both compounds are characterized by a single sharp reflection corresponding to the wave vector $q3 = 0.332\,\text{Å}^{-1} = 2\pi/18.9\,\text{Å}^{-1}$ for KI-5(2) and $q3 = 0.322\,\text{Å}^{-1} = 2\pi/19.5\,\text{Å}^{-1}$ for KI-5(3). Thus the S1 phase of the short homologues corresponds to an S_{q3} phase according to the terminology of the KI-5(4) reference compound, i.e. to an intercalated smectic structure.

Upon cooling, KI-5(3) transforms at 98°C from the S1 phase to a monotropic phase denoted S2. The orientated pattern of this S2 phase demonstrates the simultaneous existence of three resolution limited peaks in the low angle region. The corresponding diffraction vectors $q1 = 0.138\,\text{Å}^{-1} = 2\pi/45.5\,\text{Å}^{-1}$, $q2 = 0.181\,\text{Å}^{-1}$ and $q3 = 0.319\,\text{Å}^{-1} = 2\pi/19.7\,\text{Å}^{-1}$ are collinear and reflect the occurrence of an incommensurate S_{Aic} phase with two underlying incommensurate smectic modulations at $q1$ and $q3$. The ratio of the two periods $q3/q1$ is an irrational number larger than 2. The weak peak at $q2$ corresponds to a satellite which is the signature of a superlattice for this incommensurate smectic phase. The three wave vectors comply with the additivity condition $q3 = q1 + q2$, initially set for biaxial lock-ins [30], which is also satisfied in a S_{Aic} phase in which the three vectors are collinear [23].

Thus KI-5(3), in addition to KI-5(4) and KII-5(4), is the third example of a non-symmetric dimesogen which exhibits an incommensurate low ordered smectic phase. This is probably also the case for KI-5(2), but the large degree of metastability of the S2 phase prevents X-ray analysis. Note that the S1–S2 transition line can be observed through a large part of the KI-5(2)/KI-5(3) binary diagram (see later). The extrapolation of this line to pure KI-5(2) agrees with the transition temperature determined by microscopic observations.

3.1.3. *Summary*

The study of the KI-5(m) series gives three main results:

(1) The dependence of the smectic layering on the length of the terminal alkyl chain shows that the early members exhibit an S_{q3} phase, i.e. a ‘monomer-like arrangement’ involving intercalated structures, while the later homologues give an S_{q1} phase, i.e. a ‘dimer’ structure. On the contrary, we must remember the reversed evolution of the layer spacing as a function of the spacer length: short spacers give S_{q1} and long spacers S_{q3} phases [13]. In this sense it is obvious that the terminal aliphatic chain and the aliphatic spacer do not play a symmetric role in the smectic organization in such dimesogens.

(2) An incommensurate smectic S_{Aic} phase occurs for short terminal chains. It results from the coexistence of two incommensurate periodicities $2\pi/q1$ and $2\pi/q3$. Thus the occurrence of such an S_{Aic} phase first presupposes the possibility of development of an S_{q3} arrangement, and it seems that such structures are prevented from forming for long terminal chains.

(3) KI-5(4) constitutes an intermediate regime in which the system hesitates between the two periodicities and develops incommensurate and two dimensional fluid smectic phases.

3.2. *Evolution of the layering parameters through successive binary diagrams in the KI-5 (m) series*

An increase of the length of the terminal alkyl chain causes the smectic periodicity to change from $2\pi/q3$ to $2\pi/q1$: it corresponds to a d/l ratio less than 0.5 for the early members in the S_{q3} phase and d/l close to 1 in the S_{q1} phases of the longer chain compounds. This prompts the question as to how important is the molecular length in inducing such drastic modifications of the smectic layering. One way to answer this is by studying binary mixtures. Indeed, in this way the average length can be changed continuously from one extreme to the other, which is not possible through a study of pure compounds.

Binary diagrams between successive homologues were prepared to compare the smectic parameters with the average molecular length L. L is defined as the arithmetic mean of the all-*trans* molecular lengths of the two pure compounds l_A and l_B for a given composition: $L = l_A(1 - x_B) + l_B x_B$. These phase diagrams are constructed by determining for each mixture, the transition temperatures by microscopy and DSC, and the smectic parameters by X-ray analysis. To clarify the drawings we plot neither the melting lines nor the coexistence lines for the first order (or weakly first order) transitions.

Schematic X-ray patterns of the different smectic phases encountered in these phase diagrams are drawn in figure 2.

3.2.1. *Four successive binary diagrams*

KI-5(2)/KI-5(3) and KI-5(3)/KI-5(4) binary diagrams are shown as figure 3. A large smectic S_{q3}, figure 2(*a*), extends over the whole concentration range in both diagrams.

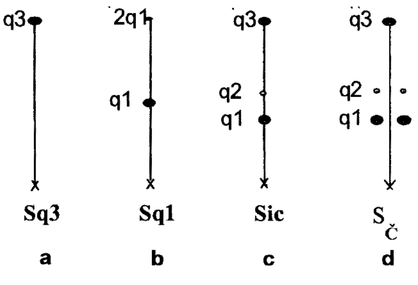

Figure 2. Schematic patterns of the smectic phases characterized by one wave vector, $q3$ (*a*) or $q1$ (*b*); or by the coexistence of two incommensurate wave vectors $q1$ and $q3$ collinear in incommensurate S_{ic} regions (*c*) and non collinear in the modulated smectic domain (*d*).

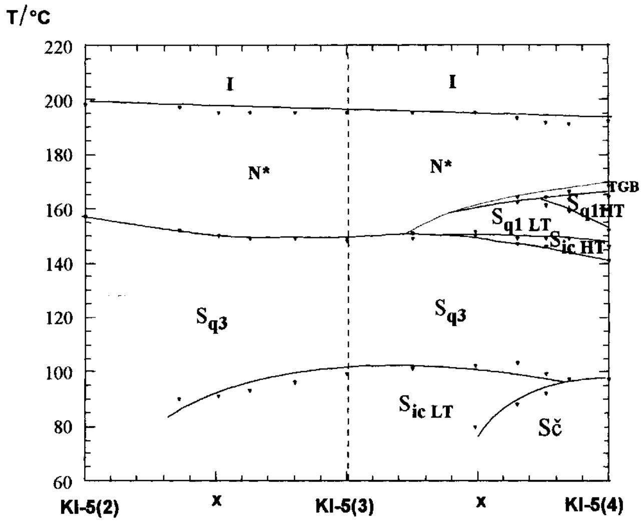

Figure 3. Juxtaposition of the temperature–concentration binary diagrams between successive short homologues: KI-5(2)/KI-5(3) and KI-5(3)/KI-5(4).

On increasing the proportion of KI-5(4) in the KI-5(3)/KI-5(4) system, commensurate S_{q1} phases appear at high temperatures, figure 2(*b*). They correspond to the TGB, $S_{q1\,\mathrm{HT}}$, $S_{q1\,\mathrm{LT}}$ phases of the KI-5(4) compound. Between the S_{q1} and S_{q3} phases, a small incommensurate $S_{ic\,\mathrm{HT}}$ domain is observed as for pure KI-5(4).

The low temperatures regions of the two phase diagrams are characterized by the existence over a large concentration range of an incommensurate fluid smectic phase $S_{ic\,\mathrm{LT}}$, figure 2(*c*), which changes into a modulated $S_{\check{c}}$ structure, figure 2(*d*), with decreasing temperature and/or increasing molecular length. Since the two S_{ic} regions are not connected it is not possible to assert that they are identical and this is why they are differently labeled. Representative X-ray patterns of three of the different phases are given in figure 4.

In the same way, figure 5 shows the KI-5(4)/KI-5(5) and KI-5(5)/KI-5(6) binary diagrams. They are dominated by the existence of the periodicity related to $q1$, that is to say connected to the dimer length. As shown in the diagrams, the S′1 phases of KI-5(5) and KI-5(6) are isomorphous with the $S_{q1\,\mathrm{LT}}$ phase of KI-5(4). In a concentration range located between KI-5(4) and the KI-5(4)–0.2 KI-5(5) mixture, an S_{q3} domain still remains and a competition between the two periodicities $2\pi/q1$ and $2\pi/q3$ occurs giving rise to the high temperature $S_{ic\,\mathrm{HT}}$ phase (figure 6). At lower temperature, this incommensurate smectic transforms into a modulated smectic phase, assigned as $S_{\check{c}}$, which keeps the same local order as the incommensurate phase.

The schematic representation of figure 7 summarizes the structural evolution of the smectic domains as a function of the average molecular length L from compounds KI-5(2) to KI-5(6).

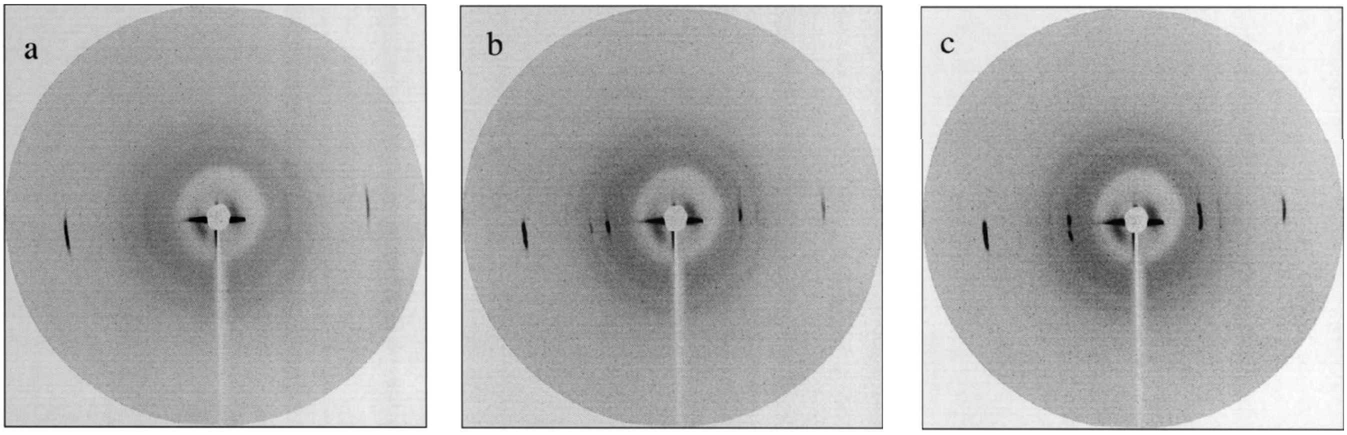

Figure 4. X-ray patterns of orientated samples of a KI-5(3)/0.5 KI-5(4) mixture (*a*) at 130°C, S_{q3} phase; (*b*) at 100°C, $S_{ic\,LT}$; (*c*) at 90°C: modulated $S_{\check{C}}$.

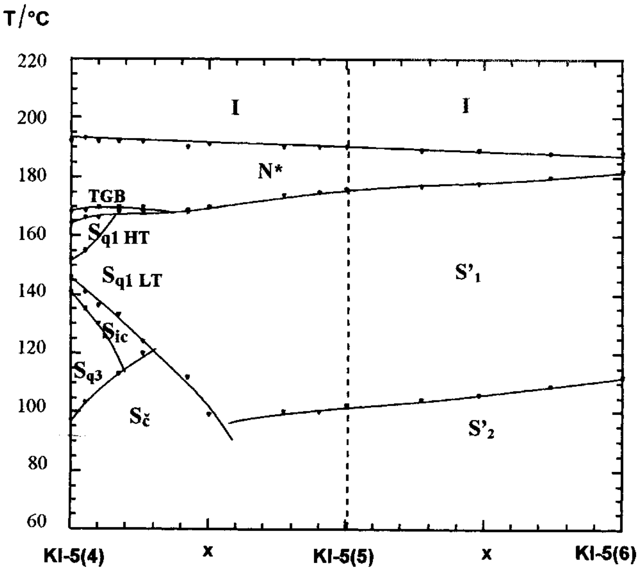

Figure 5. Juxtaposition of the temperature–concentration binary diagrams between successive long homologues: KI-5(4)/KI-5(5) and KI-5(5)/KI-5(6).

3.2.2. *Commensurate phases: 'S_{q3}' and 'S_{q1}' regimes*

Figure 8 shows the dependence of the layer spacing d on the average molecular length; the linear evolutions of the layering parameter with increasing molecular length in the S_{q3} as well as in the S_{q1} phases are immediately apparent:

In the S_{q3} phase, the layer spacing linearly increases with L. $d = 0.45L$ and thus corresponds to a smectic parameter shorter than half the molecular length. This intercalated S_{q3} phase is preserved only up to a critical average length ($L \approx 44.7$ Å).

The S_{q1} phase emerges for $L > 44.4$ Å and its smectic parameter linearly expands with L. $d \approx 0.92L$, but remains significantly shorter than the average molecular length. This latter observation suggests that the molecules which are forming the layered structure are either tilted or bent. In addition, we can note that the first harmonic $2q1$ corresponds to a layering parameter close to the extrapolation of the $q3$ periodicity.

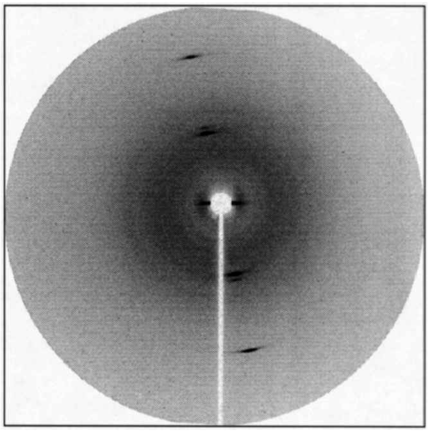

Figure 6. X-ray patterns of orientated sample of a KI-5(4)/0.1 KI-5(5) mixture at 142°C: $S_{ic\,HT}$.

These regular evolutions of the layer spacing validate the choice of the average molecular length L to describe the evolution of the smectic parameters through the successive binary diagrams.

3.2.3. *Incommensurate and modulated smectic phases*

We will now focus on the structural parameters of the smectic phases characterized by two wave vectors $q1$ and $q3$, either the incommensurate $S_{ic\,HT}$ or $S_{ic\,LT}$ phases or the modulated $S_{\check{C}}$ domain. Figure 9 summarizes the evolution of the d/L ratio in the different phases.

First we note that the periodicity connected to $q3$ is not phase dependent: the same evolution is observed for the incommensurate phases $S_{ic\,HT}$ and $S_{ic\,LT}$, the

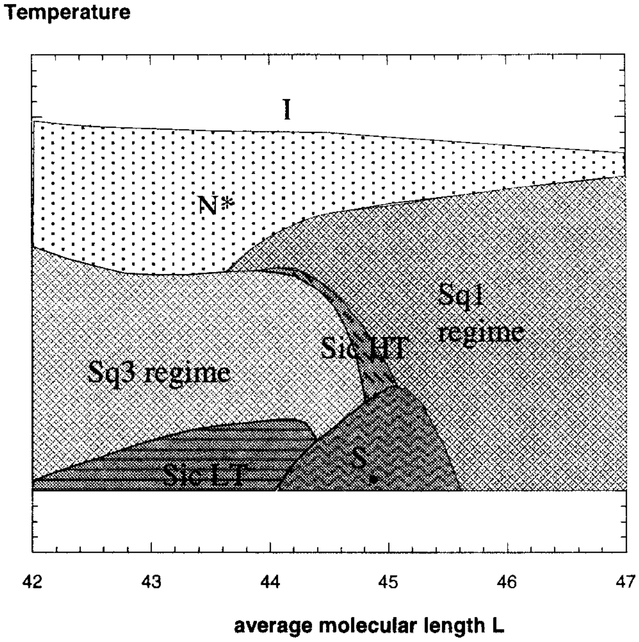

Figure 7. Schematic representation of the structural evolution of the smectic domains through the KI-5(m) series ($m = 2$ to 6) as a function of the average molecular length L.

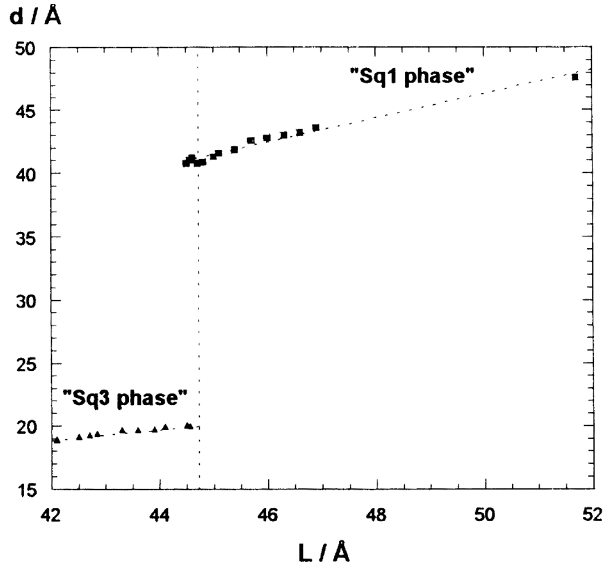

Figure 8. Evolution of the layer spacing d versus the average molecular length. S_{q1} phase corresponds to the S′1 phases of the long homologues which are isomorphous with the $S_{q1\,LT}$ phase of KI-5(4). The d value is measured ten degrees below the N*–smectic transition temperature.

modulated phase Sč and the commensurate S_{q3} phase. In all these cases the layering parameter d is locked around 0.45L. By analogy with membrane systems, this enforced periodicity probably originates from the presence of the cholesteryl moiety. It seems to be the source of anomalies in periodicity occurring in some dimesogens under study. Indeed, the existence of the periodicity connected to $q3$ is required to observe incommensurate phases or modulated phases.

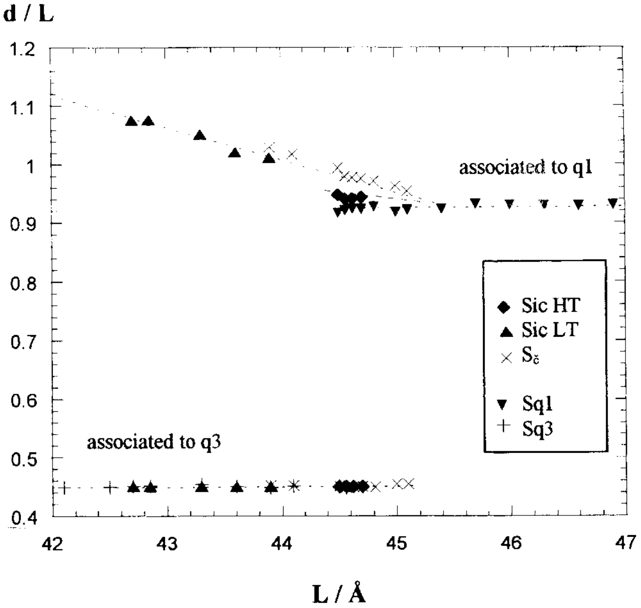

Figure 9. Evolution of the layering parameters versus the average molecular length in incommensurate and modulated smectic phases.

The evolutions of the periodicity connected to $q1$ in the incommensurate phases, as well as in the modulated Sč phase, are hence different from those observed in the commensurate S_{q1} phases. Especially, the smectic periodicity connected to $q1$ is larger than L in $S_{ic\,LT}$ and in the modulated phase. This suggests associated dimesogens with a partial overlapping. which is molecular length dependent.

The anomalies of periodicity represented by the simultaneous existence of two incommensurate wave-vectors $q1$ and $q3$ are observed up to a critical length ($L \approx 45.3$ A). They are connected with the occurrence of an incommensurate phase (either $S_{ic\,LT}$ or $S_{ic\,HT}$) up to $L \approx 44.7$ Å and extend up to $L \approx 45.3$ Å via a Sč phase while keeping the same local order. For longer L, only commensurate S_{q1} phases are observed.

3.2.4. *Tentative results from molecular modelling*

These X-ray data underline the complexity of the molecular organization; at a microscopic level several driving forces have probably to be taken into account to explain such complex structures. It is clear that the unusual mesogenic group constituted by the cholesteryl part is the key-point of these structural evolutions. Indeed, the cholesteryl moiety is able to develop preferential interactions with the aromatic mesogens as well as with alkyl chains as observed in membranes.

Computer simulations of molecular mechanics (MM) constitute an attempt to understand the molecular origin of the competing lengths or periodicities referred to earlier through the evolution of the interactions arising from different local arrangements. In MM, molecules are considered as a collection of atoms held together by elastic and harmonic forces. These forces can be described by potential energy functions which constitute the empirical force field used to reproduce the potential energy surface. Starting from an initial geometry, the energy minimization scheme makes a molecule slide down into a potential well of the energy surface. Two identical dimesogens in a minimized conformation are then associated. Both parallel and antiparallel associations of the two dimesogens have been checked, and in all cases it appears that the antiparallel association is more stable than the parallel one (about 20 kJ mol^{-1}).

We used molecular dynamics (MD) to determine configuration as a function of time. KI-5(2) and KI-5(6) antiparallel pairs were thus submitted to a 100 ps stochastic molecular dynamics run. The KI-5(2) pair remains almost unchanged during the whole run, contrary to the KI-5(6) system which exhibits a significant conformational change: after 21–22 ps a '*gauche*' conformation appears in one of the spacers and remains stable during the remainder of the run. A second attempt was made starting from a different conformation and the result was the same: the *gauche* conformation appeared after 22–23 ps and remained stable. At the end of the molecular dynamics run the electrostatic potential generated in the surrounding space by each pair of molecules was calculated and representative conformations of the KI-5(2) and KI-5(6) systems are shown in figure 10.

For both systems, one first notes the strong localization of negative potential (in blue) along the molecules, essentially centred on the COO group of the cholesteryl moiety and the O and CH=N groups of the aromatic mesogenic unit.

The overlapping obtained for the KI-5(2) antiparallel pair corresponds to a perfect matching of negative lobes with positive lobes (generated by the carbon atoms), resulting in a regular alternation of the negative and positive potentials. In this case, the characteristic length relative to $q3$, which is just less than half the molecular dimer, seems to be imposed by the cholesteryl moiety (including the COO group), while the aromatic mesogenic units with short terminal chains adapt to the layering size. The smectic order connected to $q3$ may therefore result from the favourable interactions between the different mesogenic groups.

On the other hand, with the KI-5(6) system this perfect matching of the negative and positive parts is no longer present, particularly in the spacer region. Now one can see unfavourable interactions between negative lobes (the carbonyl group of the cholesteryl moiety is in front of the oxygen atom of the aromatic moiety) due to the shortening of the spacer length which is a consequence of the *gauche* conformation. In fact these unfavourable interactions are largely counterbalanced by better van der Waals interactions between the long C6 tails and the cholesteryl moieties which explain the appearance of the *gauche* conformation. This unfavourable distribution of the electrostatic potential around half the length of the dimer may account for the loss of the length connected to $q3$ and for the development of a periodicity connected to $q1$. In addition, the bent conformation of the molecule could explain a characteristic length shorter than the molecular length.

Of course, the determination of favoured configurations of pairs of dimesogens does not allow us to describe

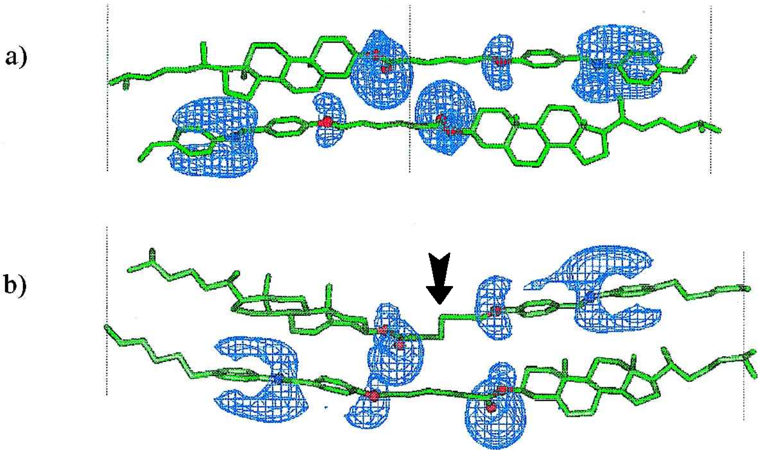

Figure 10. Representative configurations of pairs of dimesogens KI-5(2) (*a*) and KI-5(6) (*b*) in antiparallel association resulting from MD and electrostatic potential calculations. Blue contours at − 40 kJ mol^{-1}; molecules are drawn in stick representation with hydrogens omitted for clarity; O and N are represented as balls; The black arrow is pointing to the *gauche* linkage of KI-5(6); The dotted lines suggest the molecular origin of the two characteristic lengths.

the long range order in a smectic phase†. Nevertheless it underlines the difference in the local arrangement between short and long homologues which may be responsible for the different characteristic lengths. In both cases, the structure of the dimer is a result of a balance between the electrostatic and the van der Waals interactions. In the case of the short homologues, the van der Waals interactions are weak due to the short tail, and the electrostatic interactions prevail and impose a perfect matching of the positive and negative potential lobes. In the case of the long homologues, the van der Waals interactions now prevail and impose a perfect matching between the long tails and the cholesteryl moieties by means of a *gauche* conformation of one of the spacers. This in turn leads to unfavourable interactions between the negative potential lobes, the total balance being always positive.

These differences originate from a subtle equilibrium between cholesteryl–aromatic and cholesteryl–aliphatic tail interactions. For a specific aliphatic tail length corresponding to the KI-5(4) compound, several equilibrium states between the different driving forces can be observed as a function of temperature, including the occurrence of an incommensurate phase in a fluid medium. These strict molecular conditions explain the unusualness of the occurrence of incommensurate fluid smectic phases: only three examples are known and we will conclude by giving some comparisons between the three S_{ic} phases observed in these dimesogenic compounds.

3.3. *Comparison of the three examples of incommensurate smectic phases in compounds KI-5(3), KI-5(4) and KII-5(4)*

As part of a study of polar mesogens, the model of ‘frustrated smectics’ [30–33] predicted the existence of incommensurate S_{Aic} phases. Two types of relevant parameters have been considered in this phenomenological theory: elastic terms which describe modulations with preferences to order at an incommensurate wave vector, and coupling terms which favour commensurate lock-in. As a compromise between elastic and commensurability energies, two dimensional modulated antiphases or incommensurate smectic phases can occur. In this last case, two types of incommensurate S_{Aic} phases were predicted in polar systems, depending on the strength of the coupling between the two order parameters [33]: (i) a weakly coupled incommensurate phase where two penetrating smectic modulations coexist independently of each other, and (ii) a strongly coupled incommensurate soliton phase where regions with two independent wave vectors separate regions in which the two modulations are phase locked.

In the three fluid incommensurate phases that we have experimentally observed, the third reflection $q2$ is the signature of incommensurate soliton smectic structures. Nevertheless these phases differ by the intensity of the coupling between the two order parameters which depends on the ratio of the two corresponding lengths [33] [2.31 for KI-5(3), 2.54 for KII-5(4) and only 2.1 for KI-5(4)]. In the high temperature $S_{ic\,HT}$ phase illustrated by the pattern of figure 6, the two wave vectors are close and the coupling is rather strong, but due to the high temperature, the elasticity of the system allows an incommensurate smectic phase to develop. At lower temperature, the compromise between elasticity and coupling gives rise to a two dimensional $S_{\tilde{C}}$ phase.

A quantitative comparison of the three incommensurate phases can be achieved through the incommensurability parameter $\varepsilon = (q3 - 2q1)/q3$ which measures the degree of mismatch between the two wave vectors (small ε corresponds to a strong coupling, while large ε is the signature of weaker coupling).

As shown in figure 11 this parameter significantly differs for the low and high temperature incommensurate phases ($S_{ic\,LT}$ and $S_{ic\,HT}$) observed in the KI-5(m) series. In addition, the $S_{ic\,HT}$ phase probably corresponds to a tilted incommensurate phase, in agreement with a length connected to $q1$, smaller than the dimesogen length (figure 9), while $S_{ic\,LT}$ is an incommensurate smectic A.

The S_{Aic} of KI-5(3) can also be compared to the S_{Aic} of KII-5(4) previously studied [23]. The phase diagram

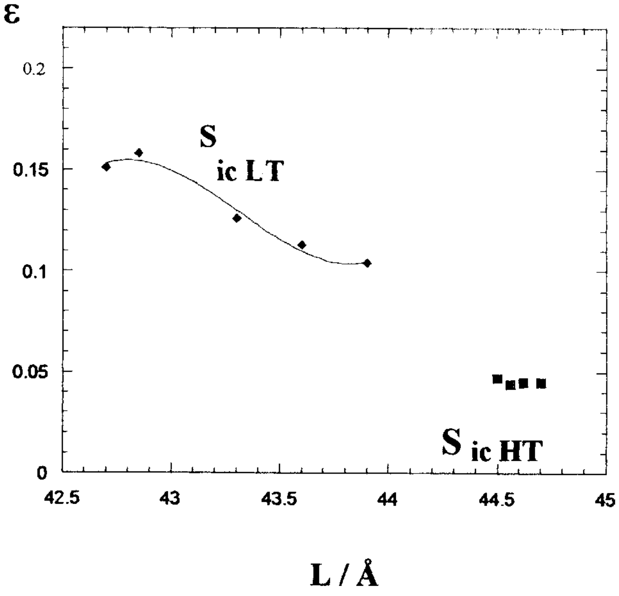

Figure 11. Evolution of the incommensurability parameter for the two incommensurate phases observed in the successive phase diagram (figure 7).

---

†Calculations including 80 dimesogens with periodic boundary conditions are currently in progress in order to gain access to a ‘bulky phase’.

reported in figure 12 shows the complete miscibility of the S_{q3} phases observed in the pure compounds, as well as of the incommensurate phases. The $q1$ and $q3$ wave vectors show regular evolutions as a function of composition and the incommensurability parameter ε increases regularly from KI-5(3) to KII-5(4), indicating a small decrease of the coupling between the two order parameters (figure 13).

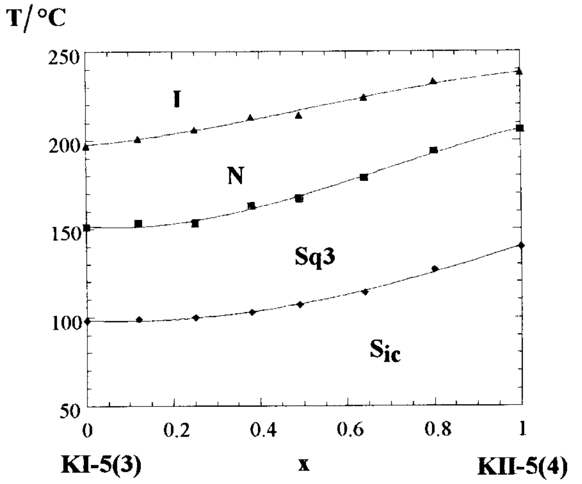

Figure 12. Temperature–concentration binary diagram between two dimesogens showing an incommensurate fluid smectic: KI-5(3) and KII-5(4). In KII-5(4) the terminal aliphatic tail is replaced by a more rigid –CH=CH–COO–C_2H_5 extremity [23].

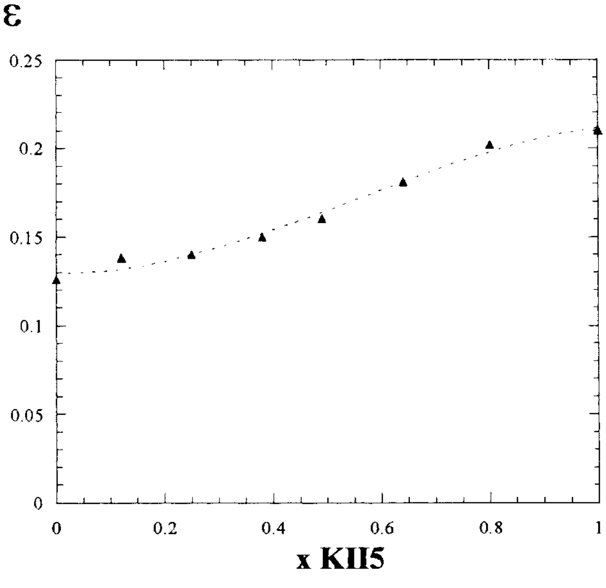

Figure 13. Regular evolution of the incommensurability parameter ε in the incommensurate phase in the KI-5(3)/KII-5(4) diagram.

4. Conclusion

The non-symmetric dimesogen series KI-$n(m)$ display two types of smectic packing. They are found to form smectic phases with a large periodicity close to the dimesogen length and/or smectic phases with a small layer spacing, lower than half the molecular length. As observed in other series [11, 14, 21, 22], the nature of the smectic packing depends on the relative length of the spacer n and of the terminal chain m, and the role of these two parts appears basically different in the KI-$n(m)$ series.

In the present study, the spacer length was fixed and the molecular length L was continuously varied by increasing the terminal chain length m through the use of binary mixtures of successive KI-5(m) homologues. Up to a critical molecular length L, anomalies of periodicity resulting from the competition between the two incommensurate lengths are observed. The systems respond to the frustration connected with this competition by forming either an incommensurate phase S_{ic} or a two dimensional modulated phase. Tentative modelling experiments show that very subtle changes in the local arrangement of the molecules are involved on varying the aliphatic tail length. For short tails, cholesteryl–aromatic associations are favoured which allow the small periodicity to develop. Increasing the aliphatic content (i.e. increasing L) favours cholesteryl–aliphatic chain interactions, progressively modifying the overlapping of the dimesogens. For long chains the possibility of obtaining the small periodicity disappears, since the association of cholesteryl–aliphatic parts is highly favoured and the large periodicity alone remains without a sublayering arrangement, and a commensurate lock-in of the two characteristic lengths systematically occurs. Thus, microscopically speaking, we highlight that the anomalies of periodicity are probably imposed by the cholesteryl part.

In terms of incommensurability, this study confirms the theoretical description of frustrated smectics. Peculiarly, the appearance of a two dimensional modulated phase constitutes an escape to an incommensurate S_{Aic} or S_{Cic} phase in the vicinity of two distinct incommensurate S_{ic} domains. Finally, a general question is raised: how can such incommensurate layering arrangements exist or be induced in other kinds of mesomorphic systems?

This collaborative research was co-sponsored by the Korea Science & Engineering Foundation and the CNRS of France.

References

[1] Hogan, J. L., Imrie, C. T., and Luckhurst, G. R., 1988, *Liq. Cryst.*, **3**, 645.

[2] Griffin, A. C., and Vaidya, S. R., 1988, *Liq. Cryst.*, **3,** 1275.

[3] Imrie, C. T., 1989, *Liq. Cryst.*, **6,** 391.

[4] Jin, J.-I., Kim, H.-S., Shin, J.-W., Chung, B. Y., and Jo, B.-W., 1990, *Bull. Korea chem. Soc.*, **11,** 209.

[5] Ikeda, T., Miyamoto, T., Kurihara, S., Tsukada, M., and Takuze, S., 1990, *Mol. Cryst. liq. Cryst.*, **182,** 357.

[6] Attard, G. S., Garnett, S., Hickmann, C. G., Imrie, C. T., and Taylor, L., 1990, *Liq. Cryst.*, **7,** 495.

[7] Jin, J.-I., Chung, B. Y., Choi, J.-K., and Jo, B.-W., 1991, *Bull. Korea chem. Soc.*, **12,** 189.

[8] Attard, G. S., Imrie, C. T., and Karasz, F. E., 1992, *Chem. Mater.*, **4,** 1246.

[9] Date, R. W., Imrie, C. T., Luckhurst, G. R., and Seddon, J. M., 1992, *Liq. Cryst.*, **12,** 203.

[10] Hardouin, F., Achard, M. F., Jin, J.-I., Shin, J.-W., and Yun, Y.-K., 1994, *J. Phys II Fr.*, **4,** 627.

[11] Attard, G. S., Date, R. W., Imrie, C. T., Luckhurst, G. R., Roskilly, S., Seddon, J. M., and Taylor, L., 1994, *Liq. Cryst.*, **16,** 529.

[12] Marcellis, A. T. M., Koudijs, A., and Sudhölter, E. J. R., 1994, *Recl. Trv. Chim.*, **113,** 524.

[13] Hardouin, F., Achard, M. F., Jin, J.-I., and Yun, Y.-K., 1995, *J. Phys II Fr.*, **5,** 927.

[14] Blatch, A. E., Fletcher, I. D., and Luckhurst, G. R., 1995, *Liq. Cryst.*, **6,** 18.

[15] Fletcher, I. D., and Luckhurst, G. R., 1995, *Liq. Cryst.*, **18,** 175.

[16] Date, R. W., Luckhurst, G. R., Shuman, M., and Seddon, J. M., 1995, *J. Phys II*, **5,** 587.

[17] Marcellis, A. T. M., Koudijs, A., and Sudhölter, E. J. R., 1995, *Liq. Cryst.*, **18,** 843.

[18] Faye, V., Nguyen, H. T., Laux, V., and Isaert, N., 1996, *Ferroelectrics*, **179,** 9.

[19] Faye, V., Barois, P., Nguyen, H. T., Laux, V., and Isaert, N., 1996, *New J. Chem.*, **20,** 283.

[20] Faye, V., Babeau, A., Placin, F., Nguyen, H. T., Barois, P., Laux, V., and Isaert, N., 1996, *Liq. Cryst.*, **21,** 485.

[21] Faye, V., Nguyen, H. T., Laux, V., and Isaert, N., 1997, *Mol. Cryst. liq. Cryst.*, **301,** 183.

[22] Faye, V., Nguyen, H. T., and Barois, P., 1997, *J. Phys. II Fr.*, **7,** 1245.

[23] Hardouin, F., Achard, M. F., Jin, J.-I., Yun, Y.-K., and Chung, S. J., 1988, *Eur. Phys J.*, **B1,** 47.

[24] Le Masurier, P. J., and Luckhurst, G. R., 1998, *Liq. Cryst.*, **251,** 63.

[25] Mohamadi, F., Richards, N. G. J., Guida, W. C., Liskamp, R., Lipton, M., Caufield, C., Chang, G., Hendrikson, T., and Still, W. C., 1990, *J. comp. Chem.*, **11,** 441.

[26] van Gunsteren, W. F., and Berendsen, H. J. C., 1988, *Mol. Simul.*, **1,** 173.

[27] Giessner-Prettre, C., 1994, *Quantum Chemistry Program Exchange*, **11,** 249.

[28] Allinger, N. L., Yuh, Y. H., and Lii, J. H., 1989, *J. Amer. chem. Soc.*, **111,** 8551.

[29] Hardouin, F., Nguyen, H. T., Achard, M. F., and Levelut, A. M., 1982, *J. Phys. Lett.*, **43,** L-327.

[30] Barois, P., Coulon, C., and Prost, J., 1981, *J. Phys. Lett.*, **42,** L-107.

[31] J. Prost, 1980, in Proceedings of the International Conference on One and Two Dimensional Order, Garmisch-Partenkirchen, 1980 (Berlin, Heidelberg, New York: Springer-Verlag), p. 125.

[32] Barois, P., 1986, *Phys. Rev. A*, **33,** 3632.

[33] Barois, P., Pommier, J., and Prost, J., 1992, *Solitons in Liquid Crystals*, edited by L. Lam and J. Prost (New-York: Springer-Verlag), p. 191.